15(*p*-[^{123}I]Iodophenyl)Penadecanoic Acid as Tracer of Lipid Metabolism: Comparison with [1-^{14}C]Palmitic Acid in Murine Tissues

Sven N. Reske, Wolfgang Sauer, Hans-Juergen Machulla, and C. Winkler

University of Bonn and University of Essen, FRG

Uptake and turnover of 15-(*p*-[^{123}I]iodophenyl)pentadecanoic acid (I-PPA), a radioiodinated free-fatty-acid analog, was examined in heart, lung, liver, kidneys, and spleen and compared with that of [1-^{14}C]palmitic acid (PA). High cardiac uptake of both I-PPA (4.4% dose/g) and PA (2.8% dose/g) was followed by a two-component tracer clearance. Kinetics of I-PPA were linked to those of PA in tissues with primary oxidation of free fatty acids or their preferential storage. Tissue lipids of all organs investigated were labeled concordantly by both tracers. Fractional distributions of PA and I-PPA incorporation in tissue lipids were significantly correlated. Thus general pathways of FFA tissue metabolism are traced by this radioiodinated free-fatty-acid analog. High-quality metabolic imaging of the heart is possible by means of I-PPA with conventional scintigraphic equipment or cross-sectional imaging with single photon emission computerized tomography facilities.

J Nucl Med 25: 1335–1342, 1984

Utilization of carbohydrates and lipids in heart muscle is closely coupled to cardiac energy production (*1*). When both substrates are present at the same time, free fatty acids are preferred to glucose under fasting conditions (*1,2*). Therefore, radiolabeled free fatty acids have been used for myocardial imaging and evaluation of cardiac fatty acid metabolism (*3–15*). Terminal phenylated as well as *p*-iodo-phenylated free fatty acids are catabolized by beta oxidation to benzoic acid (*16,17*), which is metabolized to its glucuronide and hippuric acid in the liver (*18,19*) or to the respective *p*-iodo compounds. These metabolites, along with unmetabolized benzoic or I-benzoic acid, are finally excreted with urine (*18,19*).

The purpose of this study was to compare metabolism of 15(*p*-[^{23}I]iodophenyl)pentadecanoic acid (I-PPA) with that of 1-^{14}C-labeled palmitic acid (PA), which is regarded as a reference tracer for evaluation of free-fatty-acid metabolism (*13*). A dual-tracer approach was chosen in order to establish intermediary tracer conversion in an identical metabolic environment. Tissue uptake of both tracers was compared in heart, lung, liver, kidneys, and spleen in order to analyze tracer metabolism in tissues with highly variable free-fatty-acid metabolic rates (*20*). A pulse-chase-like experimental approach was used to evaluate I-PPA and PA tissue uptake kinetics and their subsequent metabolic conversion.

Received Aug. 22, 1983; revision accepted July 13, 1984.

For reprints contact: Dr. Sven N. Reske, Institut Clin. Exp. Nuclear Medicine, Universität Bonn, Sigmund-Freud-Str. 25, 5300 Bonn 1, West Germany.

MATERIAL AND METHODS

Radiopharmaceuticals. I-PPA was produced according to the procedure described by Machulla et al. (*19,21*). Iodine-123 was produced by the ^{124}Te(*p*,2*n*)^{123}I reaction at the compact cyclotron CV 28, by irradiation of 91% $^{124}TeO_2$. I-PPA was synthetized by electrophilic iodination of 15-phenyl-pentadecanoic acid in a solution of acetic acid and concentrated sulfuric acid in the presence of sodium nitrite (*19,21*). Specific radioactivity of I-PPA was >900 Ci/mmol (*19*). [1-^{14}C]Palmitic acid

(PA) was procured commercially. Both fatty acids were dissolved in an aqueous solution of 3% human serum albumin and 10–30 mg ethanol per ml. Protein aggregates were removed from this solution by 2.2-μm millipore filtration.

Tissue distribution. All animal experiments were performed in male Wistar rats, 24-hr fasted, weighing 330 ± 50 g (mean ± s.d.). Animals were anesthetized by intraperitoneal injection of 140 ± 20 mg/kg pentobarbital 20–30 min before I-PPA and PA-application. Trachea and left external jugular vein were cannulated with polyethylene tubes (*22*). Both FFAs were injected as a bolus (250 μCi I-PPA and 2–4 μCi PA/250 μl) followed by a flush of 200 μl 0.9% saline. Duration of injection was ~10 sec. Animals were killed by insufflation of 10 ml air. The tissue specimens (heart, lung, liver, spleen, and kidneys) were rapidly removed at various time intervals after tracer injection (30 sec and 1, 2, 3, 5, 10, 20, and 30 min p.i.), rinsed with 0.9% saline, blotted on filter paper, each cut into three pieces, then weighed and frozen in liquid nitrogen. Usually this procedure was finished in 1–2 min. Six animals per time interval were examined.

Samples of the tissues were processed for liquid extraction (*17,18,19*) or placed in a test tube together with 2.0 ml distilled water. Iodine-123 radioactivity was determined in an autogamma scintillation counter. All values were corrected for radioactive decay and background radioactivity. Uptake was calculated as percentage of administered dose per g tissue, mean ± 1 s.d.

After a delay of about 4 mo, the C-14 content of the tissues and the extracted samples was measured. The samples were dissolved in 1.5 ml soluene/isopropanol mixed with 15 ml scintillation cocktail, and counted in a liquid scintillation counter together with standard samples of the injected FFA solution. Thereafter a known amount of C-14 *n*-hexadecane was added to each sample. After thorough mixing, all samples were counted again together with the standards of the FFA-albumin solution, which was prepared for counting as described above. The counting efficiency of the samples was calculated according to the internal standard method (*23*). The C-14 contents of the tissues and their fractions (% dose/g) were calculated from the efficiency-corrected sample and standard counts.

Analysis of tissue lipids. Lipid extraction from tissues was performed according to a modified method developed by FOLCH (*24,25,26*). Briefly, tissue specimens were homogenized and extracted twice with chloroform/methanol (2:1, V/V). The resulting organic, aqueous, and solid phases were separated. Radioactivity in each phase was calculated in relative units (%) or as percentage of administered dose per g tissue. Ratios between the heart and the lung "background" were calculated assuming densities of 0.55 g/cm^3 for lung tissue and 1 g/cm^3 for heart muscle (*27*). Radioactivity distribution in the organic phase was assayed as described previously (*25,26*), by thin-layer chromatography (TLC) on commercial silica F_{254} gel plates, 20 by 20 cm by 250 μm thick, together with standard lipid substances (phospholipids, cholesterol, tripalmitoylglycerides, cholesterol-ester.

I-PPA, PA, or the respective labeled lipids were identified by autoradiography. After removal of silica gel associated with the lipid fractions, their radioactivity was measured in an autogamma scintillation counter (I-PPA) or a liquid scintillation counter (PA) and calculated as percentage of injected radioactivity per g tissue. Analysis of C-14 radioactivity was performed about 4 mo after I-123 radioactivity measurements.

Imaging studies. In order to substantiate the favorable imaging properties of I-PPA for scintigraphy of the heart muscle, scintiphotos of myocardium were made from mongrel dogs about 5–10 min after i.v. I-PPA injection (2–3 mCi), using a LFOV gamma camera. A subsequent single photon emission tomogram of the heart (5 min acquisition time) was made. Experimental details have been reported (*28*).

Results. In the heart muscle, both of these fatty acids were rapidly accumulated (Fig. 1). Maximal uptake of I-PPA was 4.4% dose/g, thus exceeding that of PA (2.7% dose/g). The well-known 2-component radioactivity clearance pattern after bolus injection of radiolabeled FFA from heart muscle (*6,7,13,14*) was common to both tracers. Interestingly, a generally higher I-123 tissue

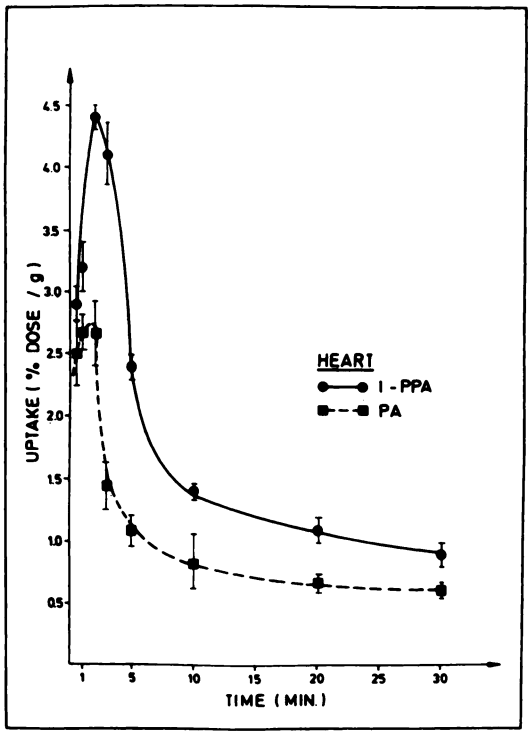

FIG. 1. Cardiac uptake of I-PPA compared with PA. ($\bar{X}$ ± s.d., N = 6 per time point)

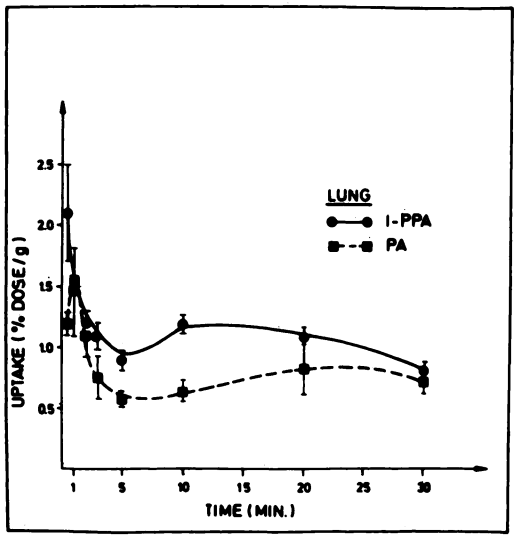

FIG. 2. Kinetics of I-PPA and PA turnover in lung tissue ($\bar{X} \pm$ s.d., N = 6 per time point)

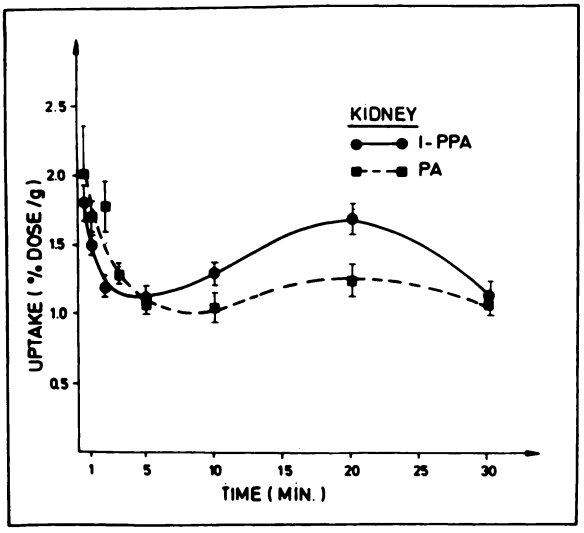

FIG. 4. Similar kinetics of I-PPA and PA in kidney ($\bar{X} \pm$ s.d., N = 6 per time point)

level was observed throughout the examination time.

In contrast to radioactivity turnover in the heart, radioactivity concentration of both FFA tracers in lung tissue decreased immediately after tracer application (Fig. 2). Following the initial clearance period, I-123 radioactivity was increased between 5–10 min after injection, whereas C-14 activity showed only a very moderate rise between 5–20 min p.i. Like the radioactivity turnover in heart muscle, I-123 concentration in the lung was generally higher (30–50%) than the C-14 content in this tissue.

In liver tissue (Fig. 3) I-PPA and PA were rapidly accumulated until 5–10 min p.i. Thereafter a slow one-component clearance of both tracers was found. Maximal I-PPA uptake was about 20% lower than maximal PA uptake. Compared with C-14, I-123 release from liver tissue seemed to be somewhat more rapid.

In spleen and kidneys, an initial clearance of radioactivity was found after tracer injection. (Figs. 5 and 6). Carbon-14 turnover in the kidneys was very similar to that of I-123 activity until 5 min p.i. Thereafter C-14 entered a plateau phase. A similar, yet somewhat lower, second phase of C-14 radioactivity was found in splenic tissue, whereas the I-123 showed a slow complex clearance pattern from the spleen.

Heart-to-lung ratios are summarized in Table 1. As assessed by the tracer content in heart and lung tissue,

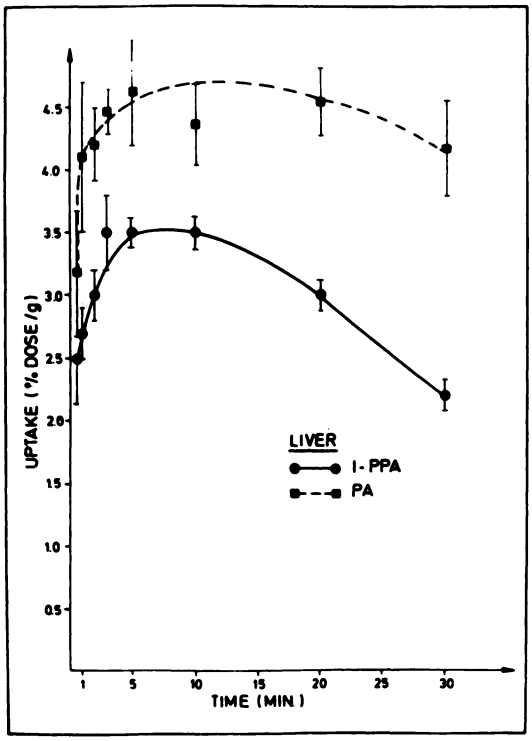

FIG. 3. Radioactivity turnover in liver tissue after I.v. I-PPA and PA injection. Note lower I-PPA uptake and more rapid I-123 radioactivity turnover. ($\bar{X} \pm$ s.d., N = 6 per time point)

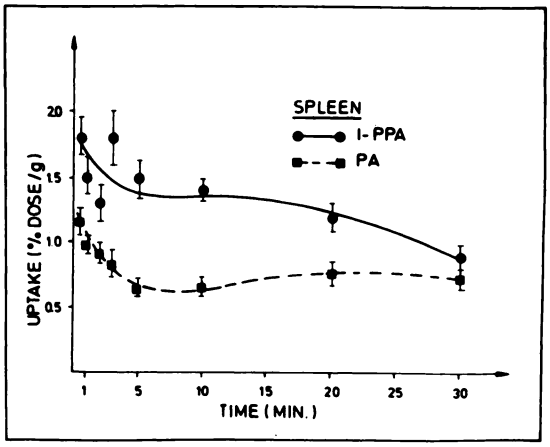

FIG. 5. Complex kinetics of I-PPA and PA in spleen. Compared with PA, a markedly increased I-PPA uptake is found in this tissue. ($\bar{X} \pm$ SD, N = 6)

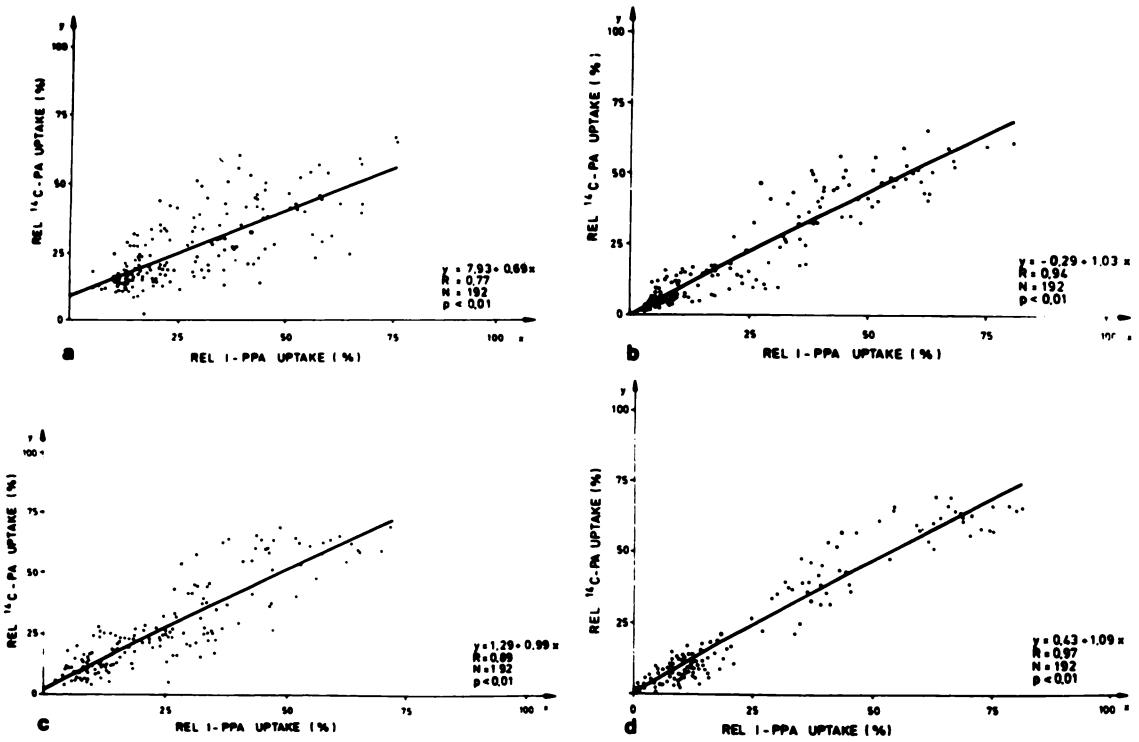

FIG. 6. Significant correlation ($p < 0.01$) between lipophilic metabolities of PA and I-PPA in heart (a), liver (b), kidney (c), and spleen (d).

I-PPA exhibited a more favorable target-to-nontarget ratio. Tissue contents of total radioactivity and of lipophilic metabolites showed a significant correlation between the two FFA tracers in all tissues investigated (Fig. 6). Radioactivity uptake into main fraction of tissue lipids (phospholipids, FFA, diglycerides, and triglycerides) was also significantly correlated (Table 3).

Imaging studies (dog). In LAO scintigrams taken between 5–10 min p.i., left-ventricular myocardium was clearly delineated (Fig. 7). Marked uptake was also observed in the liver. Myocardium-to-lung ("background") ratios, obtained in horizontal histograms from planar scintigrams of the thorax, were 1.8–2.2. Tomographic slices of the heart of a control dog and another with acute myocardial ischemia induced by ligation of left anterior descending coronary artery (LAD) 4 hr before the study (Fig. 7, lower right), showed high-contrast images of the left ventricles and visualization of the right ventricle. These images used a 40% background cutoff. The left-ventricular wall has a horseshoe shape due to imaging in a transverse plane at the level of mitral valve. Acute ischemic myocardium is clearly demarcated as an area of diminished tracer uptake; it corresponds in location—and probably also in extent—to

TABLE 1. FRACTIONAL DISTRIBUTION OF LABELED MYOCARDIAL LIPIDS AFTER ADMINISTRATION OF [1-^{14}C]palmitate (1–3), [9,10^{3}H]OLEIC ACID (*4*) OR I-PPA (*5*)

		TG*	DG	MG	FFA†	CHOL‡	PL§	animal
1. Olson et al. (*34*)		69.27	8.96	1.15	7.88	—	12.13	rat
2. Scheuer et al. (*35*)		66.27	—	6.67	7.15	—	19.73	dog
3. Crass et al. (*37*)		77.43	4.89	0.85	3.14	0.24	13.3	rat
4. Stein et al. (*36*)		80.7		—	5.6	—	13.7	rat
5. Reske et al. (*32*)	I-PPA	70–80	2–6	—	3–8	—	6–15	rat, not fasted
		45–57	10		10		17–28	rat, fasted
	PA	40–55	10		18		12–30	rat, fasted

* TG, DG, MG: tri-, di-, and monoglycerides, respectively.

† FFA: free fatty acids.

‡ CHOL: cholesterol.

§ PL: phospholipids.

TABLE 2. HEART-TO-LUNG UPTAKE RATIOS FOR I-PPA AND PA. ORGAN UPTAKE WAS NORMALIZED TO SPECIFIC GRAVITY, ASSUMING UNITY FOR HEART MUSCLE AND 0.55 FOR LUNG TISSUE (*27*)

Time after inj. (min)	0.5	1	2	3	5	10	20	30
I-PPA	2.4	4.0	6.7	6.8	4.9	2.5	2.2	2.5
PA	3.8	3.4	4.5	3.6	3.3	2.7	2.1	1.9

the hypodense area demonstrated with transmission CT after contrast infusion (Fig. 7, lower left).

DISCUSSION

After intravenous injection, rapid and substantial uptakes of PA and I-PPA were observed in the heart muscle. Maximal myocardial accumulations of 2.8 (PA) and 4.4 (I-PPA) % dose/g heart tissue were achieved within 2 minutes after tracer administration. Despite rapid tracer clearance from peripheral blood (*29*), increasing tissue concentrations in heart muscle indicated an effective extraction of the labeled FFAs from blood.

Although maximal heart uptake of I-PPA considerably exceeded that of PA, the parallel curves for cardiac tracer turnover indicated very similar global metabolism of both tracers in this tissue. The higher I-PPA heart uptake might be influenced by an altered I-PPA-to-albumin binding, a different transport rate from blood to tissue, or differences in the metabolic handling of I-PPA. Nevertheless, cardiac uptake of the 2 tracers was significantly correlated at all time points investigated, indicating a strongly related global cardiac turnover of both. A unique feature of I-PPA and PA turnover in myocardium was the rapid tracer elimination that followed the initial fast accumulation period. Similar cardiac kinetics of C-11 palmitic acid (*13–15*) or iodinated fatty acids (*6,30–32*) have been observed in a variety of experimental models.

Results reported by Machulla and Angelberger indicate identical cardiac uptake of the various FFA tracers, but slightly delayed elimination kinetics of I-PPA (*19,30*). Coenen reported similar results with Br-75 phenyl-pentadecanoic acid (*33*). However, these studies were not performed under strictly controlled physiological conditions in experimental animals, thus limiting the value of quantitative comparisons of FFA turnover.

Labeled metabolites in aqueous, solid, and lipophilic phase as well as in the subfractions of the lipid phase, were significantly correlated ($r = 0.58$, $N = 89$, $p < 0.01$). Fractional distribution of labeled cardiac lipids (Table 3) revealed a significantly concordant incorporation of both tracers into main lipid fractions—i.e., into free fatty acid (FFA), phospholipid (PL), and di- (DG) and triglyceride (TG) fractions. These findings substantiate the very similar metabolic pathways of both FFA tracers in heart muscle. Minor differences of metabolic fate of these tracers in the heart—as in other organs—include a preferential uptake of I-PPA or PA in the TG- or PL fractions, respectively (Table 3). Tissue concentrations of I-PPA- and PA-labeled cardiac lipids compared favorably with values reported for lipid uptake of C-14 or H-3-labeled free fatty acids (*34–38*). Therefore the terminal iodophenyl group does not seem to represent a major steric hindrance to I-PPA transfer in labeled lipids.

In lung tissue, moreover, a generally concordant turnover of both FFA tracers was observed. Whereas the rapid initial clearance period is probably related to the fast blood clearance of the labeled FFAs, the following plateau phase is established at a significantly higher value than in peripheral blood (1.8 compared with 4.0) (*29*). These findings indicate metabolic incorporation of a substantial fraction of the labeled FFAs into lung tissue. Frosonolo reported significant lung uptake of C-14-labeled palmitic acid, mainly into a phospholipid

TABLE 3. COEFFICIENTS OF CORRELATION BETWEEN PA AND I-PPA IN HEART, LUNG, LIVER, KIDNEY, AND SPLEEN. TOTAL ORGAN UPTAKE, RADIOACTIVITY UPTAKE INTO LIPOPHILIC METABOLITES, AND INTO LIPID SUBFRACTIONS, i.e., PL, FFA, DG, AND TG WERE ANALYZED ($N = 48$, $p < 0.01$) PER FRACTION

	Total organ uptake	Lipophilic metabolites	PL	FFA	DG	TG
Heart	0.60	0.77	0.45	0.87	0.45	0.93
Lung	0.77	0.58	0.90	0.99	0.32	0.85
Liver	0.58	0.94	0.70	0.90	0.46	0.90
Kidneys	0.48	0.89	0.73	0.95	0.44	0.67
Spleen	0.23*	0.97	0.85	0.95	0.78	0.73

* = $p < 0.05$.

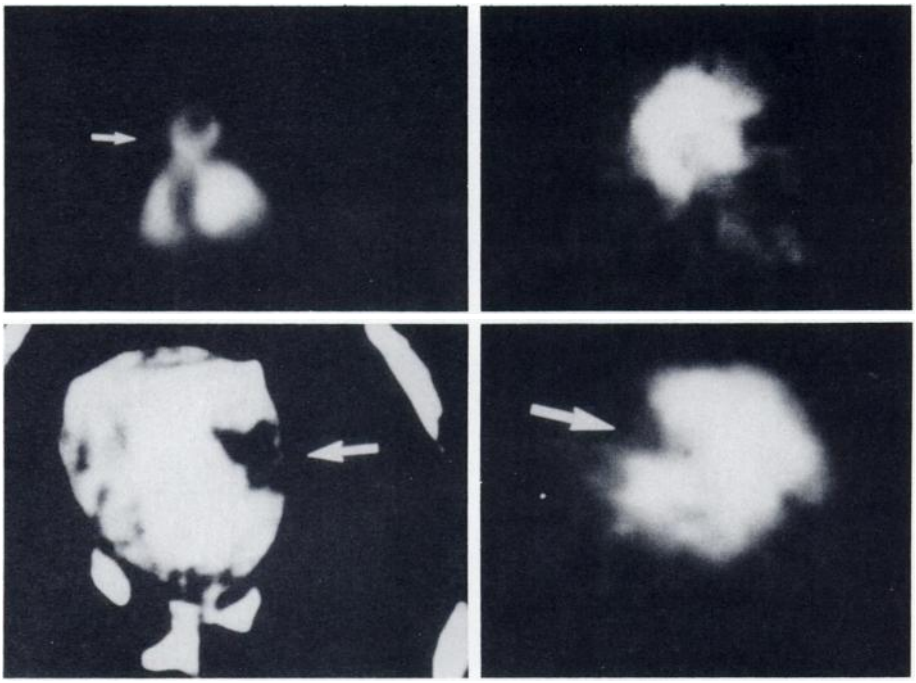

FIG. 7. Clear visualization of dog's left-ventricular myocardium 5–10 min after i.v. injection of 3 mCi I-PPA. Top left: planar scintigram recorded in 45° LAO projection (400, 000 cpm, 256 × 256 matrix). Additional tracer uptake occurred in the liver. SPECT images at mid-ventricular level of control animal (top right) and animal with acute myocardial ischemia (lower right); note clearcut demarcation of ischemic tissue (arrow), corresponding to hypodense area demonstrated on TCT image of identical animal after contrast infusion (lower left). (Laterally inverted representation of TCT is due to different reconstruction algorithm.)

with surfactant properties (*39*). Interestingly, a major uptake of both labeled FFAs into the PL fraction (about 70% of lipophilic metabolites) was found in lung tissue in our study. The slightly higher plateau value of I-123 radioactivity relative to C-14 activity between 5–20 min p.i. may be due to an increasing blood concentration of labeled hydrophilic catabolites (*40*), released from tissues with high FFA turnover rates.

Apart from heart muscle, the liver was the only tissue exhibiting an increasing PA and I-PPA uptake. In all, about 40–50% of applied dose was incorporated at maximum. These values are in general agreement with data reported by others (*41*), who found that "over 30% of injected dose" accumulated in the liver after i.v. injection of C-14-labeled palmitic acid. Whereas the slightly lower liver uptake of I-PPA remains unexplained, the somewhat faster clearance of I-123 radioactivity from the liver might be due to release of labeled hydrophilic metabolites (i.e., I-123 hippuric acid and I-123 benzoic acid glucuronide), since both substances are synthetized in and released from liver tissue (*18*,*42*). Fractional C-14 and I-123, radioactivity distribution in liver tissue showed a significant correlation (Table 3), indicating a closely related turnover of PA and I-PPA in this tissue.

Early and high radioactivity uptake of the phospholipid fraction in liver tissue was in good agreement with results of van Golde and van den Bergh, who reported that already 10–30 sec after i.p. injection of C-14-labeled glycerol, -palmitate or -oleate, the phospholipid precursor phosphatidic acid was maximally labeled in liver tissue (*41*).

In the kidneys a very similar turnover of both PA and I-PPA was encountered. Since the renal energy demand is met mostly by oxidation of FFA (*43*), the initial fast C-14 and I-123 radioactivity clearance period may be affected by tracer blood clearance, degradation of the labeled FFAs, and metabolite excretion. The second rise of I-123 content between 10 and 20 min p.i. is probably caused mainly by renal extraction of hydrophilic catabolities of I-PPA, which are excreted subsequently. Indeed, it has been shown in murine experiments and in patients that up to 70–80% of administered I-PPA was excreted into the urine during 24 hr after i.v. I-PPA injection (*19*). The lower C-14 content in the kidneys may result from concurrent $^{14}CO_2$ elimination by the lungs. In the spleen a significantly higher uptake of I-PPA was found, relative to PA. This finding, as well as elucidation of the complex clearance kinetics of both tracers, needs further investigation. The distribution of labeled lipids in the highly cellular splenic tissue should be influenced considerably by the more abundant lymphocyte and platelet membrane lipids (*44*). It has been reported that C-14-labeled palmitic acid is taken up by these cell types, mainly into the phospholipid fraction—a labeling pattern that has also been observed in our study. (PL uptake in

spleen tissue peaked at ~70% of lipid phase). We speculate that this high tracer uptake into PL fraction is related to PL uptake in cell membranes.

Linear regression analysis of PA and I-PPA uptakes in the tissues investigated and their fractions (hydrophilic and lipophilic, phase and metabolites associated with solid-tissue residues), and in the subfractions of the lipid phase (FFA, PL, DG, and TG), revealed a significant ($p < 0.01$) similarity of turnover for the two tracers. In particular, PA and I-PPA revealed concordant metabolic patterns in tissues with highly differing rates of both overall FFA oxidation and intracellular FFA transfer in complex lipids. Thus tissue turnover of I-PPA may serve as an indicator of tissue FFA metabolism under the experimental conditions investigated. Minor differences of uptake and turnover of I-PPA, relative to PA, found especially in tissues with predominant nonoxidative FFA metabolism, are of theoretical interest but probably are not of practical concern when evaluation of FFA metabolism in a tissue with primary oxidative FFA metabolism is intended.

The first scintigraphic studies performed in canine myocardium, and also in patients, showed that excellent myocardial scintigrams can be obtained by means of this tracer, both in experimental animals and man (*28,29,45,46*). This new tracer for metabolic cardiac imaging may be of potential value for detection of acute myocardial ischemia, and for the detection, location, and conceivably quantification of myocardial infarcts, especially in conjunction with single photon emission computed tomography. Promising initial clinical results in patients with coronary artery disease, studied both at rest or after supine bicycle exercise, have been reported from our laboratory (*29,45,46*).

CONCLUSION

I-PPA is taken up and metabolized in heart muscle and in the other tissues investigated in amounts comparable to those with PA. Tissue lipids were labeled concordantly by PA and I-PPA. Fractional distribution of tracer incorporation of both PA and I-PPA in tissue lipids compared favorably with results reported for H-3 or C-14-labeled palmitic acid (*34–38*). Minor differences in lipid labeling patterns comprised preferential PA uptake in phospholipids and I-PPA uptake in tissue triglycerides. Typical patterns of I-PPA and PA metabolism were observed in tissues in which free fatty acids are primarily oxidized, as in heart muscle, or are preferentially stored, as in the liver. The kinetics of I-PPA turnover were significantly related to those of PA in the tissues investigated.

In conjunction with rapid I-PPA blood clearance, high cardiac uptake, and fast oxidation of a substantial fraction of the accumulated tracer, I-PPA seems a very promising new metabolic tracer for the noninvasive evaluation of cardiac lipid metabolism. High-quality metabolic imaging of the heart is possible by means of I-PPA with conventional scintigraphic equipment, as is cross-sectional imaging with SPECT facilities.

ACKNOWLEDGMENT

* The standard lipid substances were a generous gift from Prof. Egge, Institute of Biochemistry, University of Bonn, FRG.

REFERENCES

1. NEELY JR, MORGAN HE: Relationship between carbohydrate and lipid metabolism and the energy balance of heart muscle. *Ann Rev Physiol* 34:413-458, 1974
2. NEELY JR, BOWMAN RH, MORGAN HE: Effects of ventricular pressure development and palmitate on glucose transport. *Am J Physiol* 216:804-811, 1969
3. EVANS JR, GUNTON RW, BAKER RG, et al: Use of radioiodinated fatty acids for photoscans of the heart. *Circ Res* 16:1-10, 1965
4. GUNTON RW, EVANS JR, BAKER RG et al: Demonstration of myocardial infarction by photoscans of the heart in man. *Am J Cardiol* 16:482-487, 1965
5. POE ND, ROBINSON GD, GRAHAM LS, et al: Experimental basis for myocardial imaging with ^{123}I-labeled hexadecanoic acid. *J Nucl Med* 17:1077-1082, 1976
6. MACHULLA HJ, STÖCKLIN G, KUPFERNAGEL CH, et al: Comparative evaluation of fatty acids labeled with C-11, Cl-34m, Br-77 and I-123 for metabolic studies of myocardium: Concise communication. *J Nucl Med* 19:298-302, 1978
7. FREUNDLIEB CH, HÖCK A, VYSKA K, et al: Myocardial imaging and metabolic studies with [17-^{123}I] iodoheptadecanoic acid. *J Nucl Med* 21:1043-1050, 1980
8. OTTO CA, BROWN LE, WIELAND DM, et al: Radioiodinated fatty acids for myocardial imaging: Effects of chain length. *J Nucl Med* 22:613-618, 1981
9. VAN DER WALL EE, HEIDENDAHL GAK, DEN HOLLANDER W, et al: Metabolic myocardial imaging with ^{123}I-labeled heptadecanoic acid in patients with angina pectoris. *Eur Nucl Med* 6:391-396, 1981
10. MACHULLA HJ, MARSMANN M, DUTSCHKA K: Biochemical concept and synthesis of a radioiodinated phenylfatty acid for in vivo metabolic studies of the myocardium. *Eur J Nucl Med* 5:171-173, 1980
11. KLEIN MS, GOLDSTEIN RA, WELCH MJ, et al: External assessment of myocardial metabolism with [^{11}C]palmitate in rabbit hearts. *Am J Physiol* 237:H51-H58, 1979
12. GOLDSTEIN RA, KLEIN MS, WELCH MJ, et al: External assessment of myocardial metabolism with C-11 palmitate in vivo. *J Nucl Med* 21:342-348, 1980
13. SCHELBERT HR, HENZE E, PHELPS ME: Emission tomography of the heart. *Semin Nucl Med* 10:355-373, 1980
14. SCHÖN HR, SCHELBERT HR, ROBINSON GD, et al: C-11-labeled palmitic acid for the noninvasive evaluation of regional myocardial fatty acid metabolism with positron computed tomography I. Kinetics of C-11 palmitic acid in normal myocardium *Am Heart J* 103:532-547, 1982

15. LERCH RA, BERGMANN SR, AMBOS HD, et al: Effect of flow-independent reduction of metabolism on regional myocardial clearance of C-11 palmitate. *Circulation* 65:731-738, 1982
16. KNOOP F: Der Abbau aromatischer Fettsäuren im Tierkörper. *Beitr Chem Physiol Path Braunschweig* 6:150, 1905
17. SCHMITZ B, RESKE SN, MACHULLA HJ, et al: Gas chromatographic-mass spectrometric analysis of the incorporation and the metabolism of ω-(p-iodo-phenyl-)pentadecanoic acid in the perfused rat heart. *Proceedings of the Twenty-first International Meeting, European Society of Nuclear Medicine.* Schattauer Verlag, 1984, pp 361-363
18. TUBIS M, BLAHD WH, ENDOW JS, et al: The metabolism of ortho-I-131 iodobenzoic acid. I. Its use as a possible liver function test. *J Nucl Med* 5:532-541, 1964
19. MACHULLA HJ, DUTSCHKA K, VAN BENNINGEN D, et al: Development of 15(p-^{123}I-phenyl-)pentadecanoic acid for in vivo diagnosis of the myocardium. *J Radioanal Chem* 65:279-286, 1981
20. GILBERTSON JR: Cardiac muscle. In *Lipid Metabolism in Mammals-1*, Snyder F, ed. New York, Plenum Press, 1977, pp 367-397
21. MACHULLA HJ, MARSMANN M, DUTSCHKA K: Synthesis of radioiodinated phenylfatty acids for studying myocardial metabolism. *J Radioanal Chem* 56:253-261, 1980
22. THER W: Grundlagen der experimentellen Arzneimittelforschung Stuttgart, Thieme, 1965
23. NEAME KD, HOMEWOOD CA: *Introduction to Liquid Scintillation Counting*, London and New York, Butterworths, 1974, pp. 83-115
24. FOLCH G, LEES M, STANLEY GHS: A simple method for isolation and purification of total lipids from animal tissues. *J Biol Chem* 266:497-509, 1957
25. RESKE SN, FUCHS R, MACHULLA HJ, et al: Radiochromatographic microanalysis of myocardial lipids prelabeled with radioiodinated fatty acids. *Radiochem Radioanal Lett* 55, 257-264, 1982
26. EGGE H, MURAWSKI U, MÜLLER J, et al: Mikrolipidanalysen aus Serum mit dem Eppendorf-System 3000. *Z Klin Chem Klin Biochem* 8:488-491, 1970
27. HEBEL R, STROMBERG MW: *Anatomy of the Laboratory Rat.* Baltimore, Williams and Wilkins Co., 1976, pp 59-61
28. RESKE SN, BIERSACK HJ, LACKNER K, et al: Assessment of regional myocardial uptake and metabolism of ω-(p-^{123}I-phenyl-)pentadecanoic acid with serial single-photon emission tomography. *Nucl Med Band XXI, Heft* 6:249-253, 1982
29. RESKE SN: Jod-123-Phenyl-Pentadecandäure-Ein neuer tracer zur Untersuchung des myokardialen Metabolismus freier Fettsäuren. *Der Nuklearmediziner* 1:25-46, 1983
30. ANGELBERGER P, WAGNER-LÖFFLER M, DUDCZAK R, et al: ^{123} (131)I-labeled aliphatic and aromatic fatty acids: Optimized preparation and biodistribution. In *Radioak. Isotop. in Klinik und Forschung*, 15. Int. Symp., Bad Gastein, Höfer R, Bergmann H, eds. 1980, pp 249-264
31. DAUS HJ, RESKE SN, VYSKA K, et al: Pharmacokinetics of p(^{131}I-phenyl-)pentadecanoic acid in the heart. In *Proceedings of the Thirteenth Congress of the European Society of Nuclear Medicine*, H.A.E. Schmidt, F. Wolf eds. F. K. Schattauer, 1981, pp. 108-111
32. RESKE SN, MACHULLA H-J, WINKLER C: Metabolism of 15-p(I-123-phenyl)-pentadecanoic acid (IP) in hearts of rats. *J Nucl Med* 23:P10, 1982 (abstr)
33. COENEN HH, HARMAND M-F, KLOSTER G, et al: 15(p-[^{75}Br]bromophenyl)pentadecanoic acid: Pharmacokinetics and potential as heart agent. *J Nucl Med* 22:891-896, 1981
34. OLSON RE, HOESCHEN RJ: Utilization of endogenous lipid by the isolated perfused rat heart. *Biochem J* 103:796-801, 1967
35. SCHEUER J, BRACHFELD N: Myocardial uptake and fractional distribution of palmitate-1-C-14 by the ischemic dog heart. *Metabolism* 15:945-954, 1966
36. STEIN O, STEIN Y: Lipid synthesis, intracellular transport and storage. *J Cell Biol* 36:63-77, 1968
37. CRASS MF, MCCASKILL ES, SHIPP JC, et al: Metabolism of endogenous lipids in cardiac muscle: Effect of pressure development. *Am J Physiol* 220:428-435, 1971
38. STEIN O, STEIN Y: Metabolism of fatty acids in the isolated perfused rat heart. *Biochim Biophys Acta* 70:517-530, 1963
39. FROSONOLO MF: Lung. In *Lipid Metabolism in Mammals—2.* Snyder, F ed. New York, Plenum Press, 1977, pp 1-31
40. RESKE SN, KOISCHWITZ D, REICHMANN K, et al: Cardiac metabolism of 15(p-^{123}I)-phenyl-)pentadecanoic acid after intracoronary tracer application. *Eur J Radiol* 4: 144-149, 1984
41. VAN GOLDE LMG, VAN DEN BERGH, SG: Liver, In *Lipid Metabolism in Mammals—1*, Snyder, F ed, New York, Plenum Press, 1977, pp 35-116
42. LEHNINGER AL: *Biochemie*, Weinheim, New York, Verlag Chem., 1977, p 447
43. TON JS, HUGGINS CG: Kidney. In *Lipid Metabolism in Mammals—2*, Snyder F, ed. New York, Plenum Press, 1977, pp. 39-72
44. ELSBACH P: White cells and platelets, In *Lipid Metabolism in Mammals.* Snyder F, ed. New York, Plenum Press 1977, pp 259-284
45. RESKE SN, SIMON H, MACHULLA HJ et al: Myocardial turnover of p-(I-123 phenyl)pentadecanoic acid (IP) in patients with CAD. *J Nucl Med* 23: P 34, 1982 (abst)
46. RESKE SN, NITSCH J, GRUBE E, et al: Ischemia-induced inhibition of myocardial 15(p-I-123)phenyl-pentadecanoic acid (IP) turnover in CAD. *Circulation* 68:III-70, 1983 (abstr)